Simulation of loading test for corroded reinforced concrete box culvert

Toyofumi MATSUO, Takuro MATSUMURA & Tsutomu KANAZU
Central Research Institute of Electric Power Industry, Chiba, Japan

ABSTRACT: We show experimental results and numerical examples about the relationship between mechanical performance and reinforcement corrosion by loading test of corroded specimen. Then, FEM analyses in consideration of reinforcement section area loss and a decrease in bond stress between reinforcement and concrete, can estimate the load-displacement relation of RC structures.

Keywords: RC box culvert, FEM, seismic performance, reinforcement corrosion

1 INTRODUCTION

Extensive researches are being conducted in various research organizations with a view to transition to a rational performance based design system of reinforced concrete(RC) structures.

It can hardly be said that such issues as the relationships between level of deterioration and the structural performance, and the deterioration process with respect to elapsed time are fully clarified. Instead, most of the RC structures have been designed under a tacit understanding that they are durable enough to be earthquake-resistant.

In order to develop a rational performance based design system, it is of cardinal importance to identify a performance evaluation method for aged RC structures, taking into account the relationship between the level of deterioration and the structural performance. Durability as well as structural capacities should be considered in the overall safety assessment of the structures.

With the situations mentioned above in mind we took up the case of steel corrosion in RC members as a representative example of deterioration. RC box culvert specimens, the reinforcement of which had been forcibly subjected to stray current corrosion, were tested under reversed horizontal loading. By using the experimental results we investigated the effect of steel corrosion on the mechanical behaviors of RC box culvert with particular reference to earthquake resistance properties.

2 EXPERIMENTAL INVESTIGATION ON STRUCTUAL BEHAVIOR OF CORRODED RC SPECIMEN

2.1 *Outline of the experiment*

(1) Specification of the specimens

The specimens used in the experiment were the cut-off sections of a RC box-culvert, which had been in service for 13 years as a discharge water channel (Nakamura et al.2000). The configuration of the section and the reinforcement arrangement are depicted in Figure 1. The original structure, which had been buried underground with cover soil depth of about 1m, was 2.1m in width and 2.7m in height with haunches in the corners. The design horizontal static seismic coefficient was 0.3, which rendered the structure web reinforcement-free. Concrete cores and steel samples were extracted form the specimens, the test results of which are listed in Table 1.

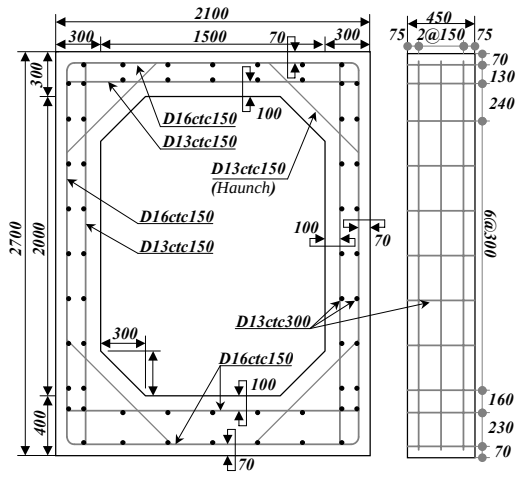

Figure 1. Section dimensions and reinforcement arrangement of the corroded specimen (Unit; mm)

Table 1 Material test results

(a) Concrete (Design strength; 24N/mm^2)

Compressive strength (N/mm^2)	Young's modulus (N/mm^2)	Tensile strength (N/mm^2)
31.5	3.29x10^4	2.68

(b) Reinforcement (Specified strength; 345 N/mm^2)

Yield strength (N/mm^2)	Yield strain (X10^{-6})	Young's modulus (N/mm^2)
381	2273	1.68x10^5

(2) Method of artificial corrosion

Appreciable deteriorations such as significant cracks and reinforcement rust were not observed in the original specimens, albeit some portions of them were subjected to change in color with shells adhered. To aggravate the corrosion condition, one of the specimens was artificially corroded using electric corrosion method. For that purpose the specimen was placed in a container filled with 3% NaCl solution so that the inner as well as outer faces of the specimen came in contact with the solution. Reinforcements and steel expanded metals were designated as anode and cathode, respectively. Direct current of 20A was imposed continuously for 16 days (See Figure 2).

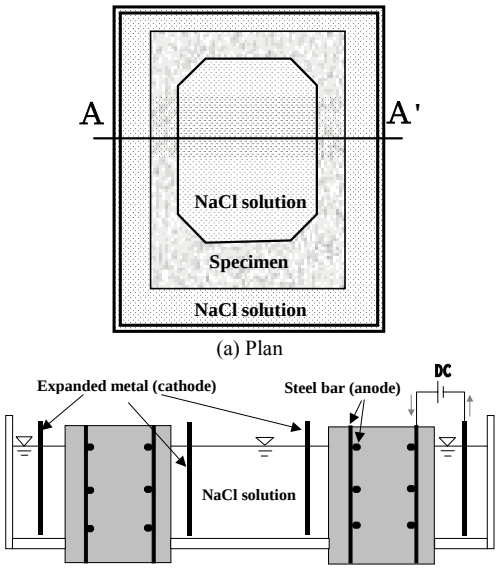

(a) Plan

(b) A-A' section

Figure 2. Electric corrosion method

(3) Loading procedures

The loading method is illustrated in Figure 3. To simulate the shear deformation mode occurring in soil during earthquakes, the specimen was reversibly loaded by two hydraulic actuators placed on the opposite sides, being controlled by displacements. Steel ingots were placed on the top of the specimen in place of over-burden soil with a thickness of 1m. The base slab was firmly clamped to the strong bed to satisfy the completely fixed condition. The load was increased stepwise repeating twice the same level of displacement (See Figure 4).

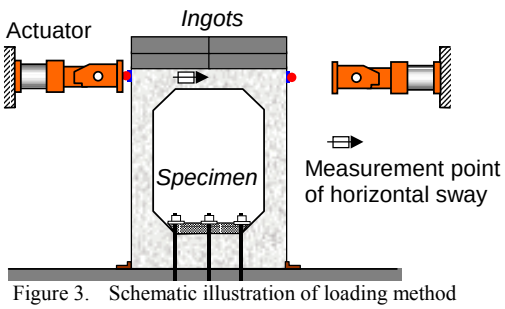

Figure 3. Schematic illustration of loading method

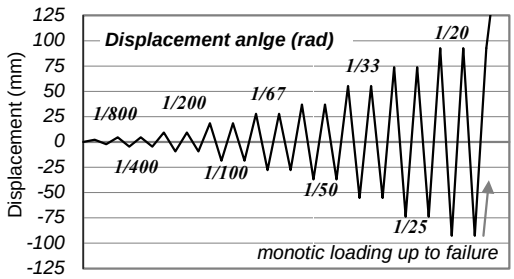

Figure 4. Loading procedures

2.2 *Experimental results and discussions*

(1) Corrosion states of steel before loading test

The crack pattern just after the electrical corrosion process is sketched in Figure 5. Major cracks appeared along the reinforcements placed close to the outer periphery of the specimen. This phenomenon may be attributed to the fact that thicker reinforcements were used in the outer periphery zone, which caused larger expansive pressure to cover concrete in spite of similar corrosion states on both sides. The maximum crack width observed was about 0.8mm.

The amount of steel corrosion was determined by two methods; one was based on the weight difference (JCI method) and the other on the strength difference. Samples of corroded steel were taken from the central portion of the specimen for which the aftereffect of loading was considered negligible. In the former test method, three coupons of reinforcement with a length of 10cm, which were extracted from each portion, were soaked in 10% ammonium di-citrate solution for three days. Then, having removed the corrosion products, the weight of each coupon was measured. The difference of the weight of the corroded sample and that of the intact steel sample, which was treated in the same way as the corroded one. For the latter test method, the reduction of steel area due to corrosion was identified as the difference between the yield strengths of corroded and non-corroded steel samples.

As is shown in Table 2, the values of corrosion varied extensively in accordance to the test methods, the portions where the samples were extracted and the diameter of steel. The amount of corrosion measured by the difference of weights represents the value averaged over a length, while that determined by the tension test corresponds to the maximum value within the tested length. It is evident that the former evaluates less corrosion than the latter. Observed phenomenon that the outer reinforcements corroded more extensively than the inner ones coincided with the measured results.

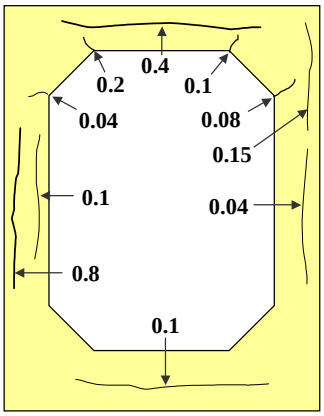

Figure 5. Crack pattern and crack width (Unit; mm)

Table 2 The measurement result of the corrosion amount

(a) Method based on the weight difference

	Outside (D16)	Inside (D13)	Average
Right side	9.09%	2.19%	5.64%
Left side	4.56%	3.82%	4.19%
Average	6.83%	3.01%	4.92%

(b) Method based on the strength difference

	Outside (D16)	Inside (D13)	Average
Right side	15.7%	9.43%	12.6%
Left side	11.9%	7.05%	9.48%
Average	13.8%	8.24%	11.0%

(2) Loading test results

Figure 6 depicts the shear deformation angle of electrically corroded specimen with respect to applied horizontal load. To compare the test results with those for the non-corroded specimen on the equal basis, the load values were converted to the case when the specimen had had a thickness of 105cm.

The maximum load of 274kN was reached when the specimen was deformed to 1% in terms of shear angle. At the second positive deformation angle of 1%, the existing corrosion crack at the mid-height of the left sidewall suddenly widened, causing a rapid load drop. When the angle reached 2%, the crack dislocated accompanying concrete spalling. In the ultimate stage shear cracks at upper and bottom regions of the right side wall became conspicuous (See Figure 7). In Figure 8 hysteretic loops of load-displacement relationships are compared for the corroded and the intact specimens. At the particular corrosion level of this experiment, the maximum load carrying capacity for the corroded specimen dropped by about 30%

in comparison to the comparable intact one. The load carrying decrement rate after the maximum load was also increased compared to the non-corroded one. It can be seen that the configuration of the hysteretic loops for the corroded specimen exhibits less energy absorbing characteristics with respect to the intact one. This may be attributed to the pronounced deterioration of bond property between steel and concrete.

A comparison of crack patterns for corroded and non-corroded specimens is sketched in Figure 9. The crack patterns of the corroded specimen seem somewhat different between right-side and left-side walls. The corrosion crack in the left-side wall opened so excessively that the cover concrete was no longer able to resist the increment of load. No apparent difference of cracking mode was observed in the right-side walls of both corroded and non-corroded specimens.

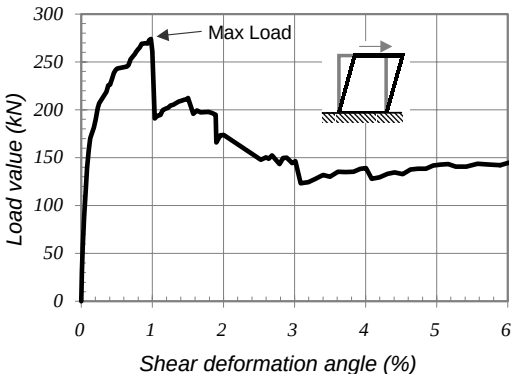

Figure 6. Skeleton curve for load-deformation relationship of the corroded specimen

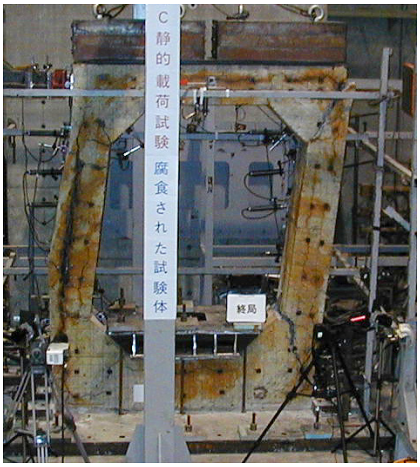

Figure 7. The ultimate failure mode of the corroded specimen

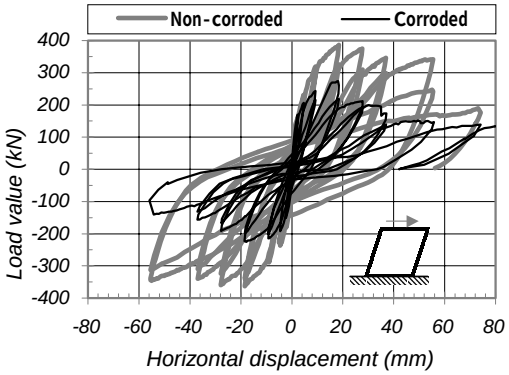

Figure 8. Comparison of the load-displacement relation for corroded and non-corroded specimens

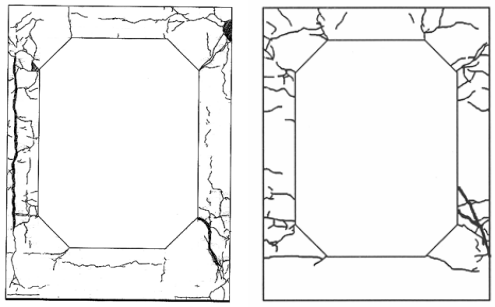

(a) Corroded specimen (b) Non-corroded specimen

Figure 9. Comparison of the crack patterns after loading test

3 ANALYTICAL INVESTIGATION USING FINITE ELEMENT METHOD

3.1 *Outline of the analysis*

In the FEM analysis we applied a smeared crack model composed of non-linear RC elements. The computer code used was the non-linear FEM program, WCOMD-SJ Ver7.1, developed by Okamura,H & Maekawa,K(1991). In this computer code the characteristics of steel concrete interface are considered as a tension softening concrete model given by Equation 1 below: (See also Figure 10).

$$\sigma_t = f_t \left(\frac{\varepsilon_{tu}}{\varepsilon_t} \right)^c \qquad (1)$$

Where f_t = concrete tensile strength; σ_t = tensile stress in concrete; ε_{tu} = strain in concrete immediately before cracking; ε_t = tensile strain in concrete; c = parameter for bond characteristics.

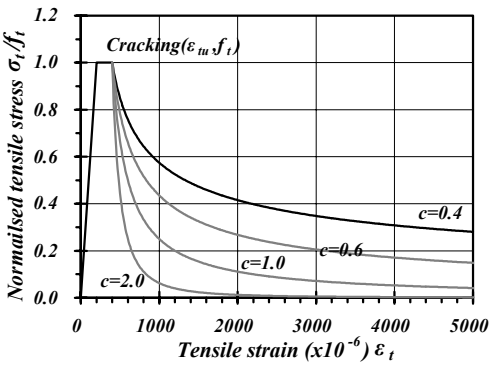

Figure 10. Tension softening model of Concrete

In this analysis, the effects of steel corrosion were taken into account by adjusting the bond parameter c as well as reduction in steel area. For the bond parameter c, 0.4 and 2.0 were adopted in the effective bond zones as recommended for deformed bars, and in the plain concrete portions to reflect the brittle behavior after cracking, respectively. The lower value of c represents the more pronounced effect of tension stiffening. The effective bond area of a reinforcing bar was evaluated by Equation 2 below:

$$l_{max} = \frac{\sqrt{\pi}}{2} D_b \sqrt{\frac{f_y}{f_t}} \quad (2)$$

Where l_{max} = side length of an equivalent square for circular effective bond area of a reinforcing bar; D_b = diameter of steel bar; f_y = yield strength of steel bar; f_t = concrete tensile strength (An, X 1996).

3.2 *Analysis applied to the RC beam tests*

(1) Analytical conditions

Prior to applying our analytical method to the box culvert specimens, we verified the validity of the analytical procedures through the comparison of analytical results with experimental ones for the corroded RC beams conducted previously. Figure 11 depicts the element mesh for the analysis. The beam was assumed to be fixed on one end, and supported on a roller on the other. Forced displacement was imposed on the two loading points. Input material properties are listed in Table 3. For the beams with known corrosion amounts, parametric study was conducted on c to identify the most suited value in terms of the best match with beam tests.

(2) Analytical results

Some examples of analytical results with experimental ones are shown in Figure 12. It can be said that if the corrosion areas are localized, deflection behavior of beams is reproduced by appropriately taking into account the bond characteristics of steel-concrete interface in addition to the reduction in steel area.

Further parameter study on c led to the c values depending on the ranges of corrosion amount as described in Table 4.

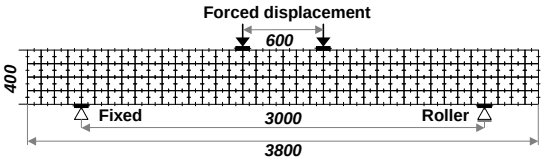

Figure 11. FEM element division figure of RC beam (Unit: N/mm^2)

Table 3 Input mechanical data for the analysis of RC beam (Unit: N/mm^2)

(a) Concrete

Compressive strength f'_c	45.3
Tensile strength f_t	3.7
Young's modulus E_c	3.06x10^4

(b) Reinforcement

Yield strength f_y	344
Young's modulus E_s	1.94x10^5

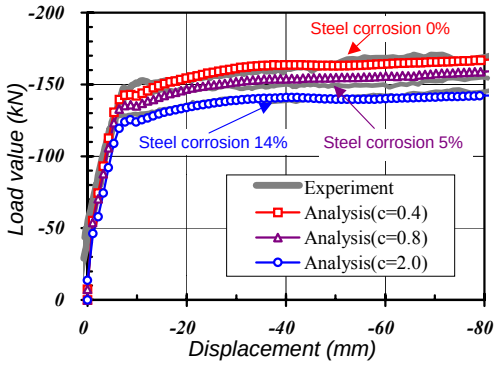

Figure 12. Comparison of the experimental and the analytical results (RC beam)

Table 4 Bond parameter values with respect to ranges of corrosion amount

Corrosion amount δW	Bond parameter c
δW≤2%	0.4
2%<δW≤5%	0.6
5%<δW≤8%	0.8
8%<δW≤10%	1.0
δW>10%	2.0

3.3 *Simulation analysis of RC culvert specimens*

(1) Non-corroded specimen

a) Analytical conditions

The FEM mesh division of the non-corroded specimen is illustrated in Figure 13. In the analysis, the base slab was assumed to be rigidly fixed, and displacement was imposed at the center of the top slab. Material input properties are listed in Table 5. Since the specimen was a part of a seawater discharge channel, which had been used for 13 years, some hair cracks were observed prior to loading. Considering these pre-existing defections and the results of preliminary analyses, tensile strength of the concrete was reduced to half of the experimentally obtained splitting tensile strength.

b) Analytical results

Analytical load-displacement relationship of non-corroded specimen is compared with the experimental one in Figure 14, which shows a good agreement each other. Also, the crack pattern predicted by analysis seems similar to that observed in the experiment (See Figure 15)

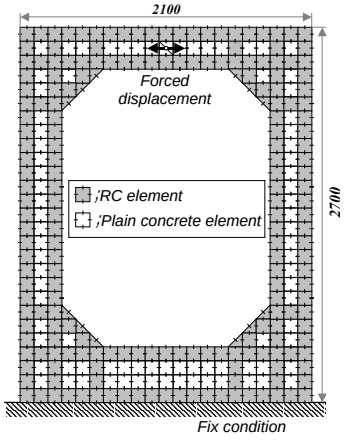

(Unit: N/mm^2)

Figure 13. FEM element division of RC box culvert

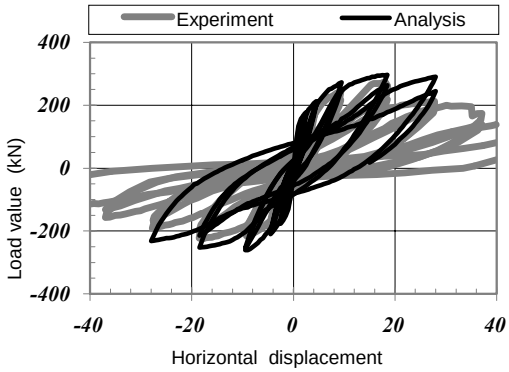

Figure 14. Analytical simulation of experiment for non-corroded specimen

Table 5 Material input data for the analysis of RC box culvert (Unit: N/mm^2)

(a) Concrete

Compressive strength f'_c	31.5
Tensile strength f_t	1.34
Young's modulus E_c	3.29x10^4

(b) Reinforcement

Yield strength f_y	381
Young's modulus E_s	1.68x10^5

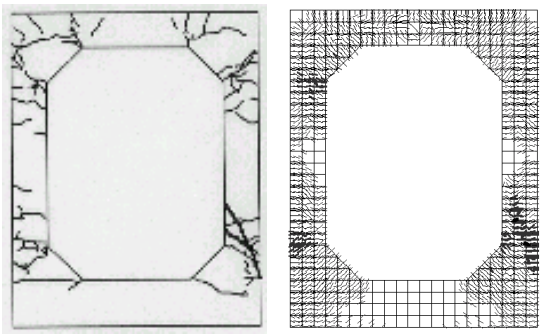

Figure 15. Comparison of experimental and analytical crack patterns for intact specimen

(2) Corroded specimen

a) Analytical conditions

To reflect the localized corrosion states in the analysis as much as possible, following conditions were assumed for the analysis. Since the yielding starts at the more corroded points of steel, not the average corrosion amount, but the value obtained by the strength difference in steel was adopted. Bond behavior is considered to be governed by the bond characteristics of steel over a length. Therefore, the bond parameter c was determined in terms of weight difference of steel. In determining the bond parameter c, distinction was made between the state prior cracking along the steel and that after appearance of cracks. In the latter state, further diversification was made depending on the crack width as summarized in Table 6. For the portions of top and bottom slabs, which do not affect the overall horizontal deformation, a constant value of average corrosion amount was assumed.

In the upper corner, an excessive diagonal crack developed towards the ultimate load, which led to reinforcement breakage. After the test the specimen was discomposed to find abnormal corrosion in this region. So, the steel area in this corner portion was arbitrarily reduced by 50% in the analysis. (See Figure 16)

Table 6 Bond parameter "*c*" identification depending on corrosion amount

Corrosion state	Bond parameter *c*
a) Before cracking along the reinforcement	
δW≤1%	0.4
1%<δW≤5%	0.5
5%<δW	0.6
b) After cracking along the reinforcement	
w≤0.1mm	0.6 (δW≤5%) 0.8 (δW>5%)
w>0.1mm	0.8 (δW≤8%)
	1.0 (8%<δW≤10%)
	2.0 (δW>10%)

Where δW: corrosion amount, *w*: Maximum crack width

b) Analytical results

Experimental results of load versus displacement relationships are compared with analytical ones in Figure 17. As can been from the figure, above mentioned sophistication of bond parameter *c* localwise led to a good agreement with the experiment. The conspicuous damage observed in the upper right corner could also be qualitatively predicted (See Figure 18).

In the actual situation, the states of corrosion in a RC structure are highly localized. The above investigation may indicate that in order to estimate the deformational as well as load carrying behavior of corroded RC members more realistically; we need to get more detailed properties and their local distributions and to incorporate them properly in the analysis.

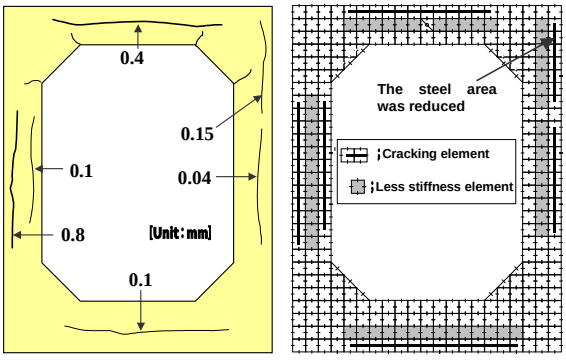

Figure 16. Cracks immediately after electric corrosion and FEM mesh division for corroded specimen

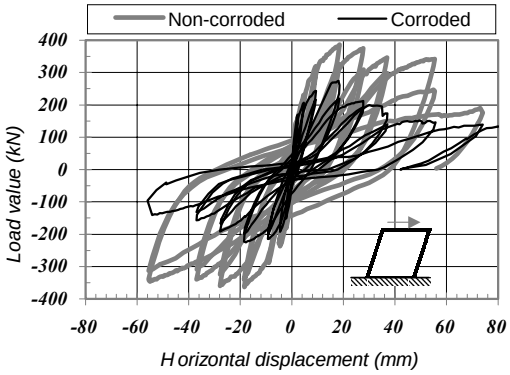

Figure 17. Experimental and analytical hyteresis for corroded specimen

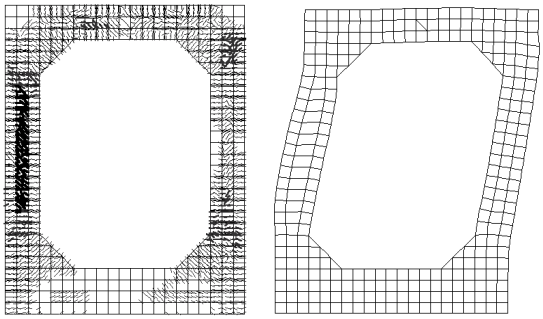

Figure 18. Analytically obtained cracking and deformation mode for corroded specimen

4 CONCLUDING REMARKS

The conclusions obtained from the study are summarized as follows;

- The artificially corroded reinforced concrete box culvert with a maximum steel corrosion amount of about 10% showed a reduction in loading capacity by approximately 30% accompanied by a less energy absorbing characteristic of load-displacement hysteresis in comparison to the non-corroded one.
- The failure mode of the corroded specimen was related to the opening of the pre-existing corrosion cracks along the main reinforcement, while that of non-corroded one was initiated by the extension of diagonal cracks in the corner.
- Based on the parametric study using the RC beam test results, the bond parameter *c*, which governs the deterioration condition of bond at steel-concrete interface to analysis, was identified. Especially when corrosion in steel extends over a wider portion of the structural member, the appropriate bond parameter should

be incorporated in the analysis in addition to the effect of section loss in steel.
- Overall horizontal load-deformation relationships of corroded RC box culvert was simulated fairly well by taking into account the bond parameter c as well as section loss in steel.
- To predict realistically the local structural distresses caused by external earthquake effects it is necessary to survey the distribution of deterioration due to corrosion, which should be properly included in the analysis.

ACKNOWLEDEMENTS

A part of the foregoing study is the joint research, which is supported by Electric Power Industry in Japan. The RC box culvert specimen was provided from Chubu Electric Power Co, Inc. for which the authors express their sincere gratitude.

REFERENCES

– An, X 1996. *Failure Analysis and Evaluation of Seismic Performance for Reinforced Concrete in Shear*, Doctor Dissertation:25-30. the University of Tokyo.
– Nakamura, H. & Tachibana, Y. & Hiramatsu, S 2000. A cyclic loading test on seismic performance by using the existing underground structure, *Electric Power Civil Engineering*: 54-58. (In Japanese)
– Okamura, H. & Maekawa, K. 1991. *Non-linear Analysis and Constitutive Laws for Reinforced Concrete Structures*. Tokyo:Gihoudou-Publishing Company Ltd.